

Metallicity distribution of ω Cen Red Giants based on the Strömgen m_1 metallicity index

A. Calamida^{1,2}, G. Bono¹, L. M. Freyhammer³, F. Grundahl⁴, C. E. Corsi¹, P. B. Stetson⁵, R. Buonanno², M. Hilker⁶ and T. Richtler⁷

¹INAF-Osservatorio Astronomico di Roma, Via Frascati 33, 00040, Monte Porzio Catone, Italy
email: calamida@mporzio.astro.it

²Universita' di Roma Tor Vergata, Via della Ricerca Scientifica 1, 00133 Rome, Italy

³Centre for Astrophysics, University of Central Lancashire, Preston PR1 2HE, UK

⁴Institute of Physics and Astronomy, Aarhus University, Ny Munkegade, 8000 Aarhus C, Denmark

⁵DAO, HIA-NRC, 5071 W. Saanich Road, Victoria, BC V9E 2E7, Canada

⁶ESO, Karl-Schwarzschild-Str. 2, D-85748 Garching bei München, Germany

⁷Universidad de Concepcion, Departamento de Fisica, Casilla 106-C, Concepcion, Chile

Abstract. We adopted *wby* Strömgen photometry to investigate the metallicity distribution of ω Cen Red Giant (RG) stars. We provided a new empirical calibration of the Strömgen $m_1 \equiv (v-b) - (b-y)$ metallicity index based on cluster stars. The new calibration has been applied to a sample of ω Cen RGs. The shape of the estimated metallicity distribution is clearly asymmetric, with a sharp cut-off at low metallicities ($[Fe/H] < -2.0$) and a metal-rich tail up to $[Fe/H] \sim 0.0$. Two main metallicity peaks have been identified, around $[Fe/H] \approx -1.9$ and -1.3 dex, and a metal-rich shoulder at ≈ -0.2 dex.

Keywords. globular clusters: general — globular clusters

1. Introduction

The intermediate-band Strömgen photometric system (Strömgen 1966; Crawford 1975) presents several indisputable advantages when compared with broad-band photometric systems such as the Johnson-Cousins-Glass (Cousins 1976). The key advantages of the Strömgen photometric system are: *i*) the possibility to provide robust estimates of intrinsic stellar parameters such as the metal abundance ($m_1 \equiv (v-b) - (b-y)$ index, Anthony-Twarog & Twarog 2000, hereinafter ATT; Hilker 2000, hereinafter H00), the surface gravity ($c_1 \equiv (u-v) - (v-b)$ index), and the effective temperature (H_β index, Nissen 1988; Olsen 1988; ATT). Furthermore, theoretical and empirical evidence (Stetson 1991; Nissen 1994; Calamida *et al.* 2005) suggest that the reddening free $[c_1] \equiv c_1 - 0.2 \times (b-y)$ index is a robust reddening indicator for HB stars hotter than 8,500 K. *ii*) Accurate Strömgen photometry can be adopted to constrain the ensemble properties of stellar populations in complex stellar systems like the Galactic bulge (Feltzing & Gilmore 2000) and the disk (Haywood 2001). *iii*) Strömgen photometry has been recently adopted to investigate the membership and the metallicity distribution of RG stars in the Local Group dwarf spheroidal galaxy Draco (Faria *et al.* 2006). Moreover, Strömgen photometry it has also been adopted to remove the degeneracy between age and metallicity in stellar systems hosting simple stellar populations (globular clusters, elliptical galaxies) and to investigate age and metallicity distribution of dwarf elliptical galaxies in the Coma and Fornax clusters (Rakos & Schombert 2005). On the other hand, the Strömgen system presents two substantial drawbacks: *i*) the u , v -bands have short

effective wavelengths, namely $\lambda_{eff} = 3450, 4.110 \text{ \AA}$. As a consequence the possibility to perform accurate photometry with current CCD detectors is hampered by their reduced sensitivity in this wavelength region. *ii*) The intrinsic accuracy of the stellar parameters, estimated using Strömgren indicators, strongly depends on the accuracy of the absolute zero-point calibrations. This typically means an accuracy better than 0.03 mag. This limit could be easily accomplished in the photoelectric photometry era, but it is not trivial at all in the CCD photometry era. Moreover and even more importantly, current empirical calibrations of the Strömgren metallicity index are based either on field stars (Anthony-Twarog & Twarog 1998) or on a mix of cluster and field stars (Schuster & Nissen 1989; H00). However, empirical spectroscopic evidence suggest that field and cluster stars present different heavy element abundance patterns (Gratton, Sneden & Carretta 2004). Moreover, the occurrence of CN and/or CH rich stars in GCs (Grundahl, Stetson, & Andersen 2002, hereinafter GSA02) along the RG (H00), the subgiant and the main sequence (Stanford *et al.* 2004; Kayser *et al.* 2006) opens the opportunity of an independent calibration of the Strömgren metallicity index only based on cluster stars as originally suggested by Richtler (1989).

2. Calibration of the Strömgren metallicity index

In order to calibrate the metallicity index m_1 we selected four globular clusters, namely M 92, M 13, NGC 1851, NGC 104, that cover a broad range in metallicity ($-2.2 < [Fe/H] < -0.7$), are marginally affected by reddening ($E(B - V) \leq 0.04$), and for which accurate Strömgren photometry well-below the Turn-Off region is available. The photometry for these clusters was collected with the 2.56m Nordic Optical Telescope and with the Danish 1.54m Telescope. The reader interested in details of the observations, data reduction and calibration procedures is referred to Grundahl *et al.* (1999, GSA02) and to Calamida *et al.* (2005, 2007, in preparation). Empirical evidence suggests that the m_1 versus color relation of RG stars presents a linear trend and a good sensitivity to iron abundance (SN88; H00). Therefore, we selected cluster stars from the tip to the base of the RGB with a photometric accuracy $\sigma_{u,v,b,y} \leq 0.03$ mag for each cluster in our sample. However, in order to avoid subtle systematic uncertainties in the empirical calibrations, current cluster RG stars need to be cleaned from the contamination of field stars. To accomplish this goal we decided to use optical-NIR color planes to split cluster and field stars. We cross-identified stars in common with our Strömgren catalogs and the Near-Infrared Two Micron All Sky Survey (2MASS) catalog (Skrutskie *et al.* 2006). We found that the best optical-NIR color-color plane to properly identify field and cluster stars is the $u - J$, $b - H$. All cluster samples were reduced by $\approx 40\%$ after the color-color plane selection. The reader interested in details concerning the cleaning procedures adopted is referred to Calamida *et al.* (2007). We derived new Metallicity-Index-Color (MIC) empirical relations that correlate the iron abundance of RG stars to their metallicity (m_1) and color (CI_s) indices.

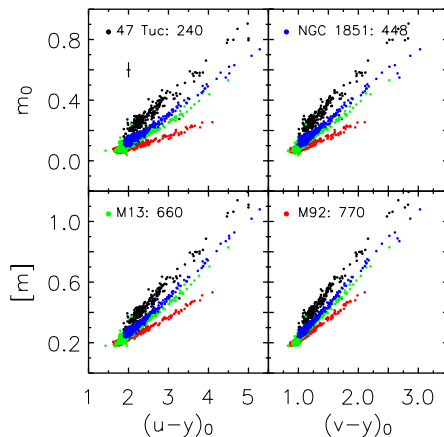


Figure 1. Candidate RG stars for the four calibrating clusters plotted in different MIC planes. Dots of different colors mark RG stars of different clusters. The error bars in the top left panel account for uncertainties both in the photometry and in the reddening correction. The number of selected RG stars in each cluster is given.

Together with the unreddened m_1 index (m_{10} , hereinafter m_0), we also derived independent empirical MIC relations for the reddening free parameter $[m] = m_1 + 0.3 \times (b - y)$. This Strömberg index was adopted to overcome deceptive uncertainties in clusters affected by differential reddening. Fig. 1 shows the cleaned samples of candidate RGs for the four calibrating clusters in four different unreddened MIC planes. We assumed $E(b - y) = 0.70 \times E(B - V)$, $E(v - y) = 1.33 \times E(B - V)$, $E(u - y) = 1.84 \times E(B - V)$, adopting the reddening law from Cardelli *et al.* (1989) and $R_V = 3.1$. Reddening values for the selected clusters are from Harris (2003) and Schlegel *et al.* (1998). The error bars plotted in the top left panel display the photometric error budget for the unreddened color indices ($\sigma(u - y)_0 \leq 0.05$, $\sigma(v - y)_0 \leq 0.045$ mag) and for the metallicity indices ($\sigma(m_0/[m]) \leq 0.05$ mag). Data plotted in Fig. 1 show two compelling empirical evidence: *i*) the $m_0/[m], CI_0$ relations are linear over a broad color range, namely $1.5 \lesssim (u - y)_0 \lesssim 5.0$ and $0.85 \lesssim (v - y)_0 \lesssim 3.0$; *ii*) the metallicity indices are well correlated with the cluster metal abundance, and indeed the four calibrating clusters present sharp and well-defined slopes. Hence, we applied a multilinear regression fit, by adopting cluster metallicities, to estimate the coefficients of the four MIC relations. Note that the metallicities adopted in the fit are in the Zinn & West (1984) scale and are based on the Calcium triplet measurements provided by Rutledge *et al.* (1997).

3. ω Cen RG metallicity distribution

We applied the new MIC relations to estimate ω Cen RGs metal abundances. In order to verify the reliability of these estimates, we cross-correlated this sample with the high-resolution spectroscopy of 40 ROA stars by Norris *et al.* (1995), finding 26 common RGs. The difference between photometric metallicities estimated adopting the $[m]$, $(v - y)_0$ MIC relation and the spectroscopic measurements are plotted versus spectroscopic abundances in Fig. 2. The error bars plotted in the figure accounts for photometric and reddening uncertainties and spectroscopic measurement errors. The agreement between photometric and spectroscopic abundances is very good, with $\Delta[Fe/H] = [Fe/H]_{phot} - [Fe/H]_{spec} \lesssim 0.3$ dex for most of the stars, and the mean of the residuals is ~ 0.02 dex. However, seven RGs (marked with an asterisk) show systematic higher photometric abundances. We found that these stars are labeled as CN-strong stars in the list of Norris. Without taking into account these peculiar stars the dispersion of the residuals is $\sigma \lesssim 0.1$ dex. Fig. 3 shows the metallicity distribution of selected ω Cen RGs, estimated adopting the m_0 , $(u - y)_0$ MIC relation. The shape of the distribution is clearly asymmetric, with a sharp cut-off at low metallicities ($[Fe/H]_{phot} < -2.0$) and a metal-rich tail up to ≈ 0.0 dex. Two main metallicity peaks can be identified around $[Fe/H]_{phot} \approx -1.9$ and -1.33 dex, and a metal-rich shoulder at $[Fe/H]_{phot} \approx -0.20$ dex. Fig. 3 shows the best fitting curve to the distribution: given the non-gaussian shape the fit has been performed adopting a convolution of three gaussians. The three gaussian curves corresponding to different stellar groups are overplotted to the distribution. The figure shows that the dispersion of the metal-poor gaussian is ≈ 0.2 dex, accounting for the photometric and the reddening uncertainties. Moreover, the lack of a resolved metal-poor tail in our ω Cen metallicity distribution suggests that these stars could have formed in a chemically homogeneous environment, as already found by Norris *et al.* (1996) based on their spectroscopic RGs metallicity distribution. However, before we can reach firm conclusions concerning our metallicity distribution we still have to constrain on a quantitative basis the dependency of the photometric abundance estimates on the occurrence of CN and CH rich stars in ω Cen.

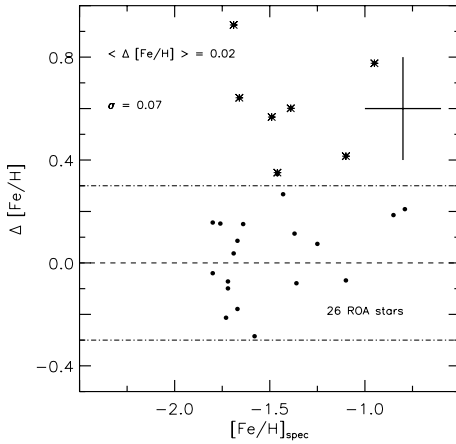


Figure 2. Difference between photometric and spectroscopic metallicities plotted versus $[Fe/H]_{spec}$ for 26 ω Cen ROA stars from the list of Norris. Asterisks mark CN-strong stars according to Norris. The error bars accounts for both photometric estimate and spectroscopic measurement errors.

References

- Anthony-Twarog, B.J., & Twarog, B.A. 1998, *AJ*, 116, 1922
 Anthony-Twarog, B.J., & Twarog, B.A. 2000, *AJ*, 120, 3111 (ATT)
 Calamida, *et al.* 2005, *AJ*, 634, L69
 Cardelli, J.A., *et al.* 1989, *ApJ*, 345, 245
 Cousins, A.W.J. 1976, *MNSSA*, 35, 70
 Crawford, D.L. 1975, *AJ*, 80, 955
 Faria, D., *et al.* 2006, *A&A*, accepted, astro-ph/0611883
 Feltzing, S., & Gilmore, G. 2000, *A&A*, 355, 949
 Gratton, R., Sneden, C. & Carretta, E. 2004, *ARA&A*, 42, 385
 Grundahl, F., *et al.* 1999, *ApJ*, 524, 242
 Grundahl, F., Stetson, P.B., & Andersen, M.I. 2002, *A&A*, 395, 481
 Haywood, M. 2001, *MNRAS*, 325, 1365
 Harris, W.E. 2003, <http://physics.physics.mcmaster.ca/harris/mwgc.dat>
 Hilker, M. 2000, *A&A*, 355, 994 (H00)
 Kayser, A., Hilker, M., Richtler, T., & Willemsen, P.G. 2006, *A&A*, 458, 777
 Nissen, P.E. 1988, *A&A*, 199, 146
 Nissen, P.E. 1994, *RMxAA*, 29, 129
 Norris, J.E., & Da Costa, G.S. 1995, *ApJ*, 447, 680
 Norris, J.E., Freeman, K.C., & Mighell, K.J. 1996, *ApJ*, 462, 241
 Olsen, E.H. 1988, *A&A*, 189, 173
 Rakos, K., & Schombert, J. 2005, *PASP*, 117, 245
 Richtler, T. 1989, *A&A*, 211, 199
 Rutledge, *et al.* 1997, *PASP*, 109, 907
 Schlegel, D.J., Finkbeiner, D.P., & Davis, M. 1998, *ApJ*, 500, 525
 Schuster, W.J., & Nissen, P.E. 1988, *A&AS*, 221, 65 (SN88)
 Schuster, W.J., & Nissen, P.E. 1989, *A&AS*, 73, 225
 Skrutskie, M.F., *et al.* 2006, *AJ*, 131, 1163, <http://www.ipac.caltech.edu/2mass/releases>
 Stanford, L.M., Da Costa, G.S., Norris, J.E., & Cannon, R.D. 2004, *MemSAIt*, 75, 290
 Stetson, P.B. 1991, *AJ*, 102, 589
 Stroemgren, B. 1966, *Ann.Rev. A&A*, 4, 433
 Zinn, R., & West, M.J. 1984, *ApJS*, 55, 45

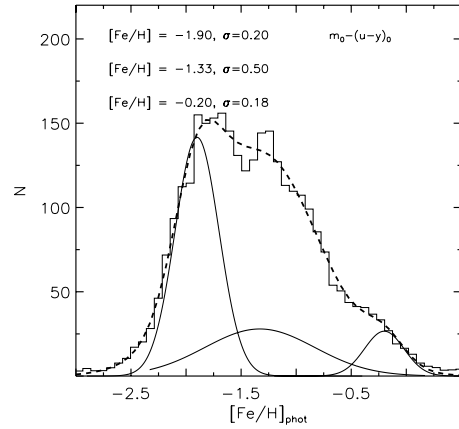


Figure 3. ω Cen RGs metallicity distribution estimated adopting the m_0 , $(u - y)_0$ empirical MIC relation. The dashed line shows the best fitting curve obtained with the convolution of three gaussians. The solid lines show the three individual gaussians. The $[Fe/H]_{phot}$ peak values and relative dispersions are also labeled.